

Electronic interlayer coupling in the LTT phase of $\text{La}_{1.79}\text{Eu}_{0.2}\text{Sr}_{0.01}\text{CuO}_4$

M. Hücker

Brookhaven National Laboratory, Upton, New York 11973-5000, USA

(Dated: November 10, 2018)

The electronic interlayer transport of the lightly doped antiferromagnet $\text{La}_{1.79}\text{Eu}_{0.2}\text{Sr}_{0.01}\text{CuO}_4$ has been studied by means of magneto-resistance measurements. The central problem addressed concerns the differences between the electronic interlayer coupling in the tetragonal low-temperature (LTT) phase and the orthorhombic low-temperature (LTO) phase. The key observation is that the spin-flip induced drop in the c -axis magneto-resistance of the LTO phase, which is characteristic for pure $\text{La}_{2-x}\text{Sr}_x\text{CuO}_4$, dramatically decreases in the LTT phase. The results show that the transition from orthorhombic to tetragonal symmetry and from collinear to non-collinear antiferromagnetic spin structure eliminates the strain dependent anisotropic interlayer hopping as well as the concomitant spin-valve type transport channel. Implications for the stripe ordered LTT phase of $\text{La}_{2-x}\text{Ba}_x\text{CuO}_4$ are briefly discussed.

PACS numbers: 74.72.Dn, 74.25.Fy, 74.25.Ha, 61.50.Ks

I. INTRODUCTION

Due to their layered structure high- T_c superconductors such as $\text{La}_{2-x}\text{Sr}_x\text{CuO}_4$ have strongly anisotropic properties. The electronic conductivity perpendicular to the CuO_2 planes is between two and four orders smaller than in the planes, and the effective interlayer superexchange about five orders weaker than the Cu-O-Cu in-plane superexchange.^{1,2,3} Nevertheless, a finite electronic interlayer coupling is essential for 3D antiferromagnetic (AF) order or 3D bulk superconductivity (SC) to occur.⁴ La_2CuO_4 has been an ideal playground for experimental and theoretical studies of interlayer interactions.^{2,5,6,7,8,9} It is amenable to doping and offers examples where a small modification of the crystal structure can change the ground state. Particularly interesting is the case of $\text{La}_{2-x}\text{Ba}_x\text{CuO}_4$ with $x \simeq 1/8$, where bulk SC is suppressed and replaced by a static order of charge and spin stripes.^{10,11,12,13} Concomitant with stripe order a transition from LTO to LTT is observed.¹⁴ There is growing evidence that the stripe ordered LTT phase causes an electronic decoupling of the CuO_2 planes.^{15,16,17,18,19} The complexity of the involved electronic, magnetic, and structural interactions, however, poses a challenge for an unambiguous experimental analysis.

Therefore, the focus of the present work lies on lightly doped samples ($x < 0.02$), where the influence of structure and magnetism on the electronic transport may be deciphered more easily. There is no SC or long range stripe order involved, and the AF order is commensurate as long as one does not cool below the spin glass transition.²⁰ Early magneto-resistance and magnetization measurements on La_2CuO_4 , and more recently on $\text{La}_{1.99}\text{Sr}_{0.01}\text{CuO}_4$ have shown that in the LTO phase the electronic interlayer transport depends on how the AF sublattices are stacked along the c -axis.^{2,7,21,22} Here, similar magneto-resistance experiments on a $\text{La}_{1.79}\text{Eu}_{0.2}\text{Sr}_{0.01}\text{CuO}_4$ single crystal are reported. This compound exhibits the same sequence of structural transitions as $\text{La}_{1.875}\text{Ba}_{0.125}\text{CuO}_4$, thus pro-

viding the opportunity to analyze the electronic interlayer coupling in the lightly doped LTT phase.

The paper is organized as follows. In the next section the experimental methods are described. The results are presented in Sec. III. There are three parts with focus on the crystal structure, the magneto-transport, and complementary magnetization measurements. In Sec. IV it is shown how these properties are connected and enable an interpretation of the electronic interlayer transport in the LTT phase. At the end of this section implications for $\text{La}_{2-x}\text{Ba}_x\text{CuO}_4$ are pointed out.

II. EXPERIMENT

The $\text{La}_{1.79}\text{Eu}_{0.2}\text{Sr}_{0.01}\text{CuO}_4$ single crystal with a diameter of \varnothing 5 mm was grown by the travelling-solvent floating-zone method in an atmosphere of flowing oxygen gas at a pressure of $p(\text{O}_2) = 5$ atm. As grown the crystal contains a considerable amount of excess oxygen, which was removed by annealing in Ar at 900°C for 24 h. The electric resistance ρ of bar shaped samples was measured with the four terminal method for currents I and magnetic fields H applied perpendicular and parallel to the CuO_2 planes. The leads were attached with silver epoxy, carefully cured to reduce the contact resistance.

The x-ray diffraction experiments were performed at beamline X22C of the National Synchrotron Light Source at a photon energy of 8.9 keV. Scattering vectors $\mathbf{Q} = (h, k, \ell)$ are specified in units of $(2\pi/a, 2\pi/b, 2\pi/c)$, where a , b and c are the lattice parameters of the orthorhombic unit cell.²³ At room temperature $a = 5.35$ Å, $b = 5.42$ Å, and $c = 13.05$ Å, while at 20 K in the LTT phase $a = b = 5.38$ Å, and $c = 13.0$ Å. The experiment was performed in reflection geometry on a polished surface which, due to twinning in the orthorhombic phase, is normal to either $[1, 0, 0]$ or $[0, 1, 0]$.

The static magnetization $M(H)$ at constant temperatures and the static susceptibility $\chi(T) = M(T)/H$ at constant magnetic fields were measured with a SQUID

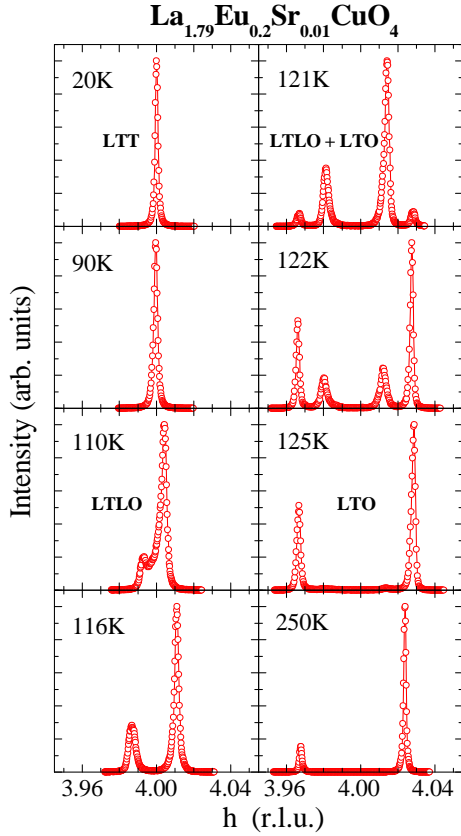


FIG. 1: (color online) Scans through the $(4, 0, 0)/(0, 4, 0)$ Bragg reflections of the two twin domains of the crystal at different temperatures.

(superconducting quantum interference device) magnetometer. All studied crystal pieces are twinned in the ab -plane, i.e., when measuring along the orthorhombic in-plane axes one averages over domains with the a and b axes interchanged. The degree of twinning was determined for each sample by bulk magnetization measurements and will be indicated wherever of relevance. Data with dominant contribution of the a -axis (b -axis) will be indexed with a^+ (b^+).

III. RESULTS

A. Crystal structure

Single crystal x-ray diffraction experiments were performed since the interpretation of the transport measurements requires a detailed knowledge of the structure. At high temperature²⁴ $\text{La}_{1.79}\text{Eu}_{0.2}\text{Sr}_{0.01}\text{CuO}_4$ transforms from the high-temperature tetragonal (HTT) phase with space group $I4/mmm$ to the LTO phase with space group $Bmab$. This transition also occurs in $\text{La}_{2-x}\text{Sr}_x\text{CuO}_4$.^{25,26} However, the Eu-doped compound shows a second transition at T_{LT} from LTO to LTT with space group $P4_2/ncm$. The nature of these transitions

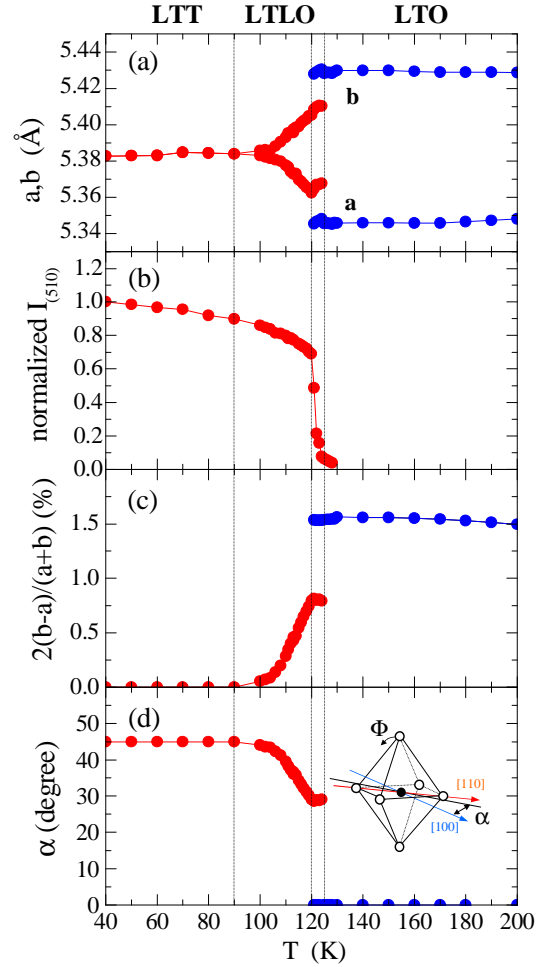


FIG. 2: (color online) Structural transition $\text{LTO} \leftrightarrow \text{LTLO} \leftrightarrow \text{LTT}$. (a) Lattice parameters a and b . (b) Normalized sum of the integrated intensities of the $(5, 1, 0)$ and $(-1, 5, 0)$ twin domain reflections. (c) Orthorhombic strain $2(b - a)/(a + b)$ in percent of the average in-plane lattice constant. (d) Calculated in-plane rotation α of the octahedral tilt axis with respect to its direction, $[1, 0, 0]$, in the LTO phase. See inset.

has been discussed in numerous studies.^{14,23,27,28,29} In first approximation all phases can be described by different pattern of tilted CuO_6 octahedra, parameterized by the tilt angle Φ and the tilt direction α , measured as the in-plane angle between the tilt axis and the $[100]$ direction, see Fig. 2(d). In the HTT phase $\Phi = 0^\circ$. In the LTO phase $\Phi > 0^\circ$ and $\alpha = 0^\circ$, while in the LTT phase $\Phi > 0^\circ$ and $\alpha = 45^\circ$. Φ is on the order of several degree and approximately the same in the LTO and LTT phase. Thus, the major change at the $\text{LTO} \rightarrow \text{LTT}$ transition is a 45° rotation of the tilt axis. Note that in the LTT phase α changes sign from plane to plane, i.e., the tilt axes in adjacent layers are orthogonal. There have been questions about whether lightly doped $\text{La}_{1.8-x}\text{Eu}_{0.2}\text{Sr}_x\text{CuO}_4$ becomes truly tetragonal, or assumes the low-temperature less-orthorhombic (LTLO) phase with space-group $Pccn$,

which is an intermediate phase between LTO and LTT with $0^\circ < \alpha < 45^\circ$.^{27,30,31} The following results will clarify this point.

Figure 1 shows scans through the $(4, 0, 0)/(0, 4, 0)$ reflections. Above 125 K there is only one pair of reflections, i.e., the sample is in the LTO phase. Upon cooling two additional peaks with reduced split appear, indicating a coexistence of the LTO and the LTLO phase. Below 120 K the transformation towards LTLO is completed. The orthorhombic strain quickly decreases and below 90 K the crystal is in the LTT phase. A summary of the temperature dependence of some structural properties is given in Fig 2. Panel (a) shows the lattice parameters a and b , panel (b) the sum of the integrated intensity of the $(5, 1, 0)/(-1, 5, 0)$ super structure reflections which are allowed in the LTLO and LTT phases only. Figure 2(c) shows the orthorhombic strain $2(b - a)/(a + b)$, and Fig. 2(d) calculated values for $\alpha = 0.5 \cdot \arccos[(b - a)/(b_0 - a_0)]$, where b_0 and a_0 are the lattice parameters in the LTO phase just above the structural transition. In the LTO phase α was set zero. The x-ray diffraction results clearly demonstrate that the low temperature transition in $\text{La}_{1.79}\text{Eu}_{0.2}\text{Sr}_{0.01}\text{CuO}_4$ is a sequence of two transitions: a discontinuous $\text{LTO} \leftrightarrow \text{LTLO}$ transition and a continuous $\text{LTLO} \leftrightarrow \text{LTT}$ transition. The temperature range of the LTLO phase is very sensitive to excess oxygen, and likely to shrink under more reducing annealing conditions.

B. Resistance

Figure 3(a) shows the c -axis resistivity $\rho_c(T)$ for different magnetic fields $H \parallel c$. The overall trend is an insulating behavior. However, the magnetic field dependence reveals some dramatic changes as a function of temperature. Above the Neel temperature of $T_N = 248$ K the field dependence is very small. Between T_N and T_{LT} a strong decrease of ρ_c with increasing H is observed. Finally, in the LTT phase the field dependence is again small. Right at the transition one can see that $\rho_c(0T)$ decreases on cooling, while $\rho_c(7T)$ increases by an equal amount. This shows that the c -axis transport in the LTT phase is distinct from both the zero field and the high field regime in the LTO phase. Interestingly, the average $[\rho_c(0T) + \rho_c(7T)]/2$ shows no significant change at T_{LT} suggesting that primarily the magnetic scattering dependent transport is affected by the structural transformation.

The nature of the changes ρ_c undergoes at the structural transition for $H \parallel c$ is even more obvious in the magneto-resistance curves in Fig. 4. In the AF ordered LTO phase $\rho_c(H)$ shows a sharp drop which grows with decreasing temperature and reaches $\sim 35\%$ at 130 K, Fig. 4(a). This is so to speak the normal behavior that is also observed in the AF ordered LTO phase of pure $\text{La}_{2-x}\text{Sr}_x\text{CuO}_4$.^{2,22} It is well established, that the effect is connected to the *spin-flip* transition at H_{SF} which

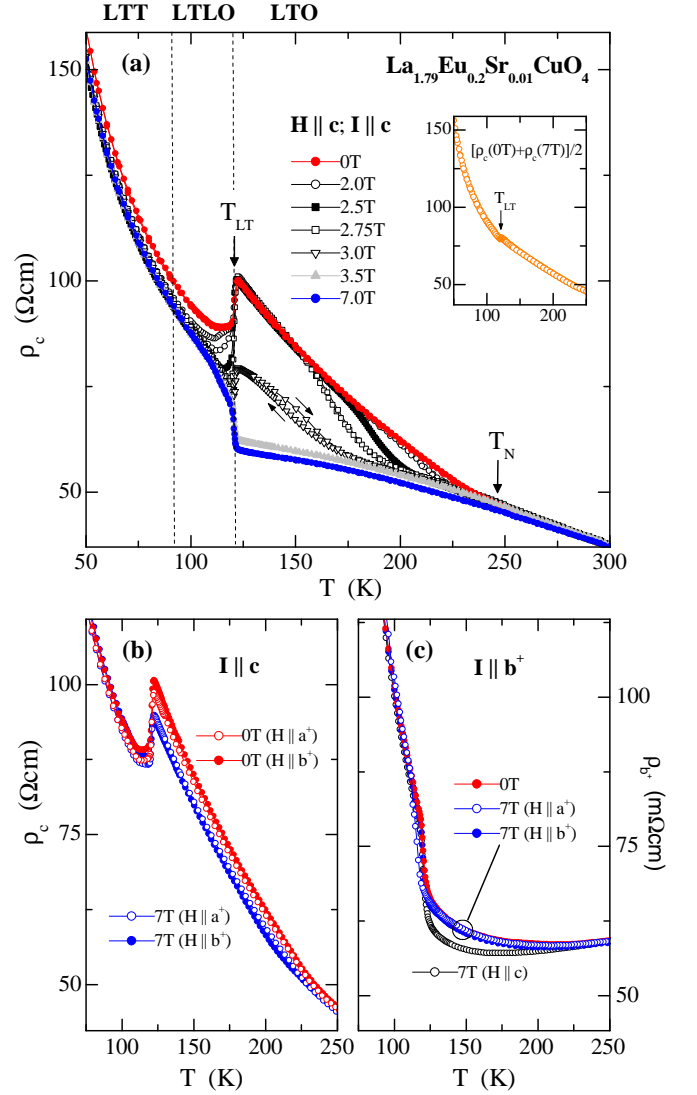


FIG. 3: (color online) c -axis and ab -plane resistivity as a function of temperature for different directions of the magnetic field. (a) ρ_c for $H \parallel c$. The inset shows the average of the 0 T and 7 T data sets. (b) ρ_c for $H \parallel a^+$ and b^+ . (c) ρ_{b^+} for $H \parallel a^+$, b^+ , and c .

alters the spin structure along the c -axis.² Corresponding magnetization data for $\text{La}_{1.79}\text{Eu}_{0.2}\text{Sr}_{0.01}\text{CuO}_4$ will be discussed in Sec. III C. The new observation is that, in the LTLO and LTT phases, this jump in $\rho_c(H)$ quickly decreases, becomes hysteretic, and at $T = 40$ K amounts to $\sim 5\%$ only, Fig. 4(b). A microscopic interpretation is given in Sec. IV.

A much weaker field dependence of ρ_c was observed for $H \parallel a^+$ and $H \parallel b^+$. Note that the crystal used for the ρ_c measurements is largely detwinned, i.e., for 80% of the sample $b^+ \parallel b$. Figure 3(b) compares $\rho_c(T)$ for $H = 0$ T and 7 T. Figure 5 compares $\rho_c(H)$ for all three field directions at $T = 130$ K in the LTO phase and at $T = 80$ K in the LTT phase. In the LTO phase a negative magneto-resistance of several percent at 7 T is observed,

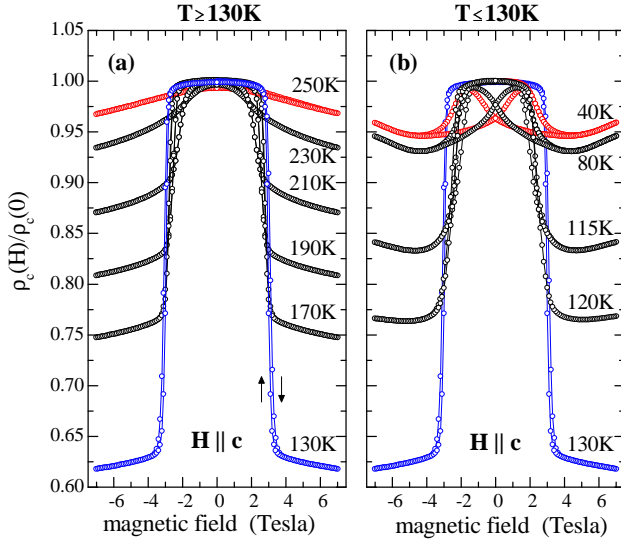


FIG. 4: (color online) Magneto-resistance $\rho_c(H)$ at different temperatures. (a) In the LTO phase. (b) In the LTLO and LTT phases and at 130 K.

which is slightly larger for $H \parallel b^+$ than for $H \parallel a^+$, consistent with results for $\text{La}_{1.99}\text{Sr}_{0.01}\text{CuO}_4$.²² In the LTT phase this weak magneto-resistance decreases by one order of magnitude. It is well known that in La_2CuO_4 and in $\text{La}_{1.99}\text{Sr}_{0.01}\text{CuO}_4$ a *spin-flop* with concomitant features in the magneto-resistance occurs for $H \parallel b$ and critical fields up to 20 T, depending on the temperature.^{3,22,32} In Ref. 33 it was suggested that the spin-flop field may decrease substantially in the LTT phase. Based on the current data one can safely say that at least up to 7 T no spin-flop takes place in the LTT phase of $\text{La}_{1.79}\text{Eu}_{0.2}\text{Sr}_{0.01}\text{CuO}_4$.

Measurements of the in-plane resistivity ρ_{b+} are presented in Fig. 3(c). The crystal used here is only slightly detwinned, i.e., for 55% of the sample $b^+ \parallel b$. At zero field $\rho_{b+}(T)$ shows a minimum at 200 K and a sharp increase at the LTO→LTLO transition. For $H \parallel a^+$ and $H \parallel b^+$ the magneto-resistance at 7 T is very small and barely visible in the T -dependent data. Field loops $\rho_{b+}(H)$ at fixed temperature show a negative magneto-resistance of less than 1% at 7 T in the LTO phase and a one order of magnitude smaller effect in the LTT phase (not shown).

For $H \parallel c$ a significant decrease of $\rho_{b+}(T)$ is observed in the AF ordered LTO phase, reaching 8% at 130 K and 7 T, see Fig. 3(c). Furthermore, the field loops $\rho_{b+}(H)$ show the same type of sharp drop at H_{SF} as for $\rho_c(H)$ and $H \parallel c$, just much smaller (not shown). In the LTT phase the magneto-resistance is again extremely small. Intuitively it is not obvious why, in the LTO phase, the in-plane resistivity should decrease at a transition that effects how the spin sublattices are staggered along the c -axis, but leaves the in-plane spin structure unchanged. The first explanation that comes to mind is that, because of the extreme anisotropy $\rho_c/\rho_{ab} \sim 10^3$, a minor misalignment of the crystal or of the contacts caused an

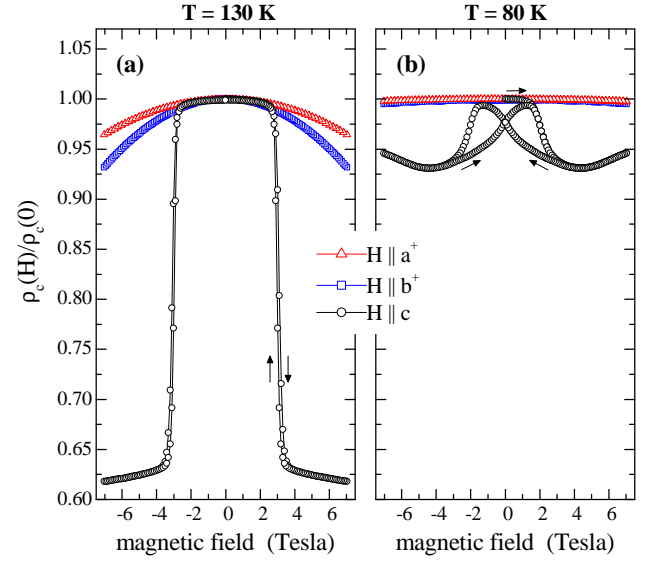


FIG. 5: (color online) Magneto-resistance $\rho_c(H)$ for $H \parallel a^+$, b^+ , and c . (a) In the LTO phase at $T = 130$ K. (b) In the LTT phase at $T = 80$ K.

admixture of a c -axis component. Since the crystal for ρ_{b+} was quite small we cannot rule out this source of error. On the other hand, similar observations have been reported for the LTO phase of $\text{La}_{2-x}\text{Sr}_x\text{CuO}_4$.^{22,34} In recent theoretical studies the effect was ascribed to a less anisotropic localization length in the high field regime ($H > H_{\text{SF}}$).^{7,35} It was suggested that this results in a more 3D like variable-range-hopping, making more out-of-plane states available for ab -plane transport. Assuming this is true, it is clear from the present data that this channel and, thus, ρ_{b+} become independent of $H \parallel c$ in the LTT phase, because as the spin-flip induced magneto-resistance of ρ_c disappears, so does the associated change of the c -axis localization length.

C. Magnetization

The magnetization measurements were performed on a bulky $m = 0.6$ g single crystal. Note that similar measurements on a $\text{La}_{1.8}\text{Eu}_{0.2}\text{CuO}_4$ crystal and on $\text{La}_{1.8-x}\text{Eu}_{0.2}\text{Sr}_x\text{CuO}_4$ polycrystals have been discussed in Ref. 33. The present sample is our first lightly doped crystal and features very sharp transitions. The presentation of data will be limited to $H \parallel c$, since no significant effects have been observed for $H \parallel ab$ and fields up to 7 T, consistent with the absence of significant magnetic field effects in ρ_{b+} .

Figure 6(a) presents the static susceptibility $\chi(T)$ for different $H \parallel c$. The Van Vleck susceptibility $\chi_{\text{VV}}^c(\text{Eu}^{3+})$ of the europium ions provides by far the largest contribution (solid line). Figure 6(b) shows the same data after subtraction of $\chi_{\text{VV}}^c(\text{Eu}^{3+})$, which can now be compared to pure $\text{La}_{2-x}\text{Sr}_x\text{CuO}_4$. For $H = 1$ T a sharp Néel peak

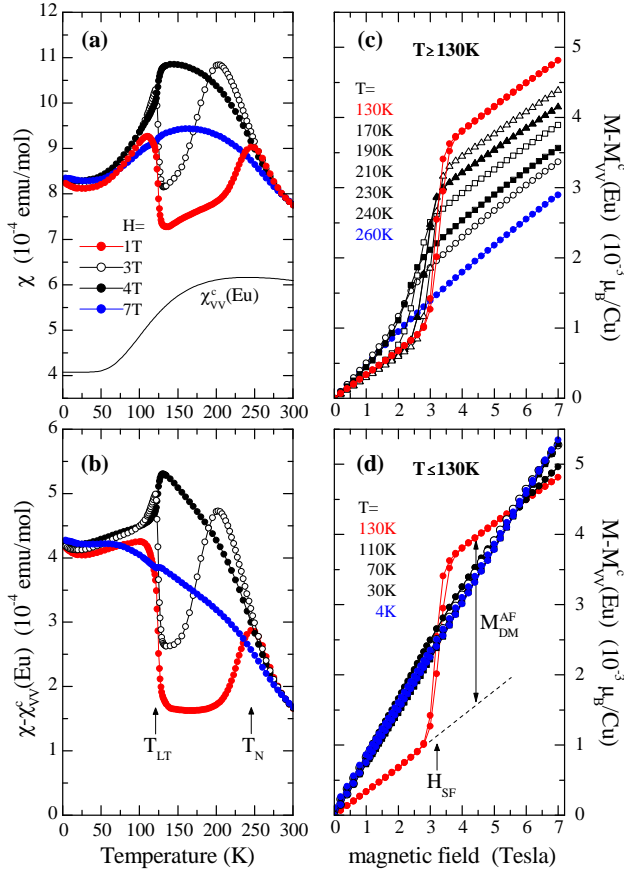


FIG. 6: (color online) (a) Static susceptibility $\chi(T)$ for different $H \parallel c$. (b) After subtraction of the Van Vleck contribution $\chi_{VV}^e(\text{Eu})$ of the europium ions. Right: Magnetization $M(H)$ after subtraction of the linear europium contribution $M_{VV}^e(\text{Eu})$. (c) In the LTO phase. (d) In the LTLO and LTT phases and at 130 K.

at T_N and a jump at T_{LT} are observed. For $H = 3$ T and higher fields the susceptibility in the AF ordered LTO phase starts to increase significantly. The same behavior is observed in La_2CuO_4 .^{33,36} In contrast, in the LTLO and LTT phases the susceptibility is elevated at any field and shows almost no field dependence. At $H = 7$ T the susceptibility increases monotonous with decreasing T .

As is well documented, the Néel peak is the fingerprint of a weak spin canting perpendicular to the CuO_2 planes, caused by Dzyaloshinsky–Moriya (DM) superexchange.^{2,8,21,37} Each plane carries a weak ferromagnetic moment (WFM) which orders antiparallel in adjacent layers for $T < T_N$. When the external field $H \parallel c$ exceeds the spin-flip field H_{SF} , needed to overcome the interlayer coupling J_\perp , the spin lattice of every other layer rotates by $\theta = 180^\circ$, with the effect that the WFM of all planes become parallel to the field. As a result the susceptibility in the LTO phase increases. Note that this is the reason why for $H = 3$ T the peak does not represent T_N , but the temperature below which $H_{SF} > H$ and WFM start to order antiparallel.

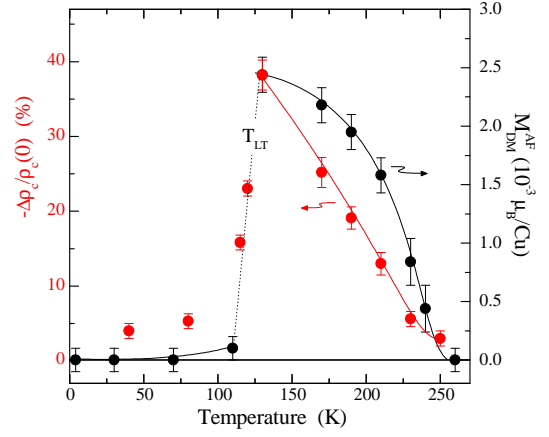


FIG. 7: (color online) Resistivity drop $\Delta\rho_c = \rho_c(7T) - \rho_c(0T)$ in percent of $\rho_c(0T)$ and magnetization jump M_{DM}^{AF} at the spin-flip transition. See Fig. 6(d) for definition of M_{DM}^{AF} . Note that M_{DM}^{AF} is only the AF ordered part of the WFM. This part becomes zero in the LTT phase, whereas the total size of the WFM does not change at the transition.³³

The changes across the LTO \leftrightarrow LTLO \leftrightarrow LTT transition are also apparent in the magnetization curves $M(H)$. The data in Figs. 6(c) and 6(d) are after subtraction of the linear Eu^{3+} Van Vleck contribution. In the LTO phase the spin-flip transition grows sharper and larger for $T < T_N$. Again, this is the normal behavior found in $\text{La}_{2-x}\text{Sr}_x\text{CuO}_4$.^{21,22} In contrast, below the structural transition no spin-flip transition is observed. The $M(H)$ curves are close to being linear in the studied field range, indicating a significant change of the magnetic coupling between the planes. Close to T_{LT} the magnetization at maximum field in the LTO and LTT phase differs only slightly. The susceptibility at 7 T in Fig. 6(b) shows even better that there is no significant anomaly at the LTO \leftrightarrow LTLO \leftrightarrow LTT transition. This implies that the WFM do not change their size across the transition, and at 7 Tesla are ferromagnetically aligned in all three phases. There is a small number of interesting theoretical studies on this new magnetic state, motivated by experiments on $\text{La}_{2-y}\text{Nd}_y\text{CuO}_4$.^{9,38} However, the static magnetization presented in Fig. 6 and in Ref. 33 seems to escape these earlier calculations, in particular with respect to the structure dependence of the $M(H)$ curves and the saturation field and moment of the WFM in the LTT phase.³⁹

Figure 7 compares the resistivity drop $\Delta\rho_c = \rho_c(7T) - \rho_c(0T)$ with the moment change M_{DM}^{AF} at the spin-flip transition. In the LTO phase the data are qualitatively the same as for $\text{La}_{2-x}\text{Sr}_x\text{CuO}_4$,^{2,22} whereas in the LTLO and LTT phase one can see the dramatic drop of these quantities. Note that M_{DM}^{AF} reflects the AF coupled part of the WFM only. The total WFM, which also consists of a non-spin-flip part (in particular in the LTT phase), continues to grow on cooling (cf. Fig. 22 in Ref. 33).

IV. DISCUSSION AND CONCLUSIONS

In several theoretical studies, motivated by the experiments on La_2CuO_4 and $\text{La}_{1.99}\text{Sr}_{0.01}\text{CuO}_4$, it was pointed out that the electronic transport between the CuO_2 planes does not depend on the direction of the weak ferromagnetic moments, but on the relative orientation θ of the spin $S = 1/2$ sublattices in neighbor planes.^{3,7,35} The apparent reason is that holes in an anti-ferromagnet prefer to hop between sublattices with same spin direction. As is shown schematically in Fig. 8 for the LTO phase, this implies that interlayer hopping at low fields ($\theta = 0^\circ$) takes place predominantly along the b -axis, whereas above the spin-flip field ($\theta = 180^\circ$) it takes place predominantly along the a -axis. The negative c -axis magneto-resistance then requires that, microscopically (not measured), the interlayer hopping resistance along a in the high-field regime is smaller than along b in the low-field regime ($\rho_\perp^a < \rho_\perp^b$). An intuitive explanation for this is that $a < b$, although the details are known to be more complicated.^{7,35}

In the LTT phase the situation is quite different (Fig. 8). The octahedral tilt axes have rotated by $\alpha = \pm 45^\circ$ in adjacent layers. The magnetization measurements on $\text{La}_{1.8-x}\text{Eu}_{0.2}\text{Sr}_x\text{CuO}_4$ presented here and in Ref. 33, as well as neutron diffraction experiments on $\text{La}_{1.7}\text{Nd}_{0.3}\text{CuO}_4$ in Ref. 30 show that, due to DM superexchange, spins follow the alternating rotation of the tilt axes. This means that spins are canted out-of-plane, but now form a non-collinear spin structure. Both the tetragonal symmetry ($a = b$) and the non-collinear spin structure ($\theta = 90^\circ$) cause a frustration of the interlayer superexchange, resulting in the absence of a well-defined spin-flip in the $M(H)$ curves, see Fig. 6(d). Moreover, the two sketched LTT spin configurations with antiparallel (left) and parallel (right) alignment of the WFM are energetically nearly equivalent, and should both populate the ground state.³⁹

What are the consequences for the c -axis magneto-transport in the LTT phase? Because $a = b$ and $\theta = 90^\circ$, both interlayer hopping directions are structurally and magnetically equivalent. Moreover, the application of a high magnetic field $H \parallel c$ has no effect on θ , although it shifts the magnetic ground state towards the one in the right panel with parallel WFM. Hence, the LTT phase is expected to be "spin-valve" inactive, consistent with the dramatic decrease of the magneto-resistance in Fig. 3(a) and Fig. 4(b).

The remaining magneto-resistance of ρ_c for $H \parallel c$ and its field hysteresis at low temperatures, Fig. 4(b), still lack interpretation. It is unclear whether these features are intrinsic or due to structural imperfections of the LTT phase, resulting from a limited domain size and LTLO or LTO like domain boundaries.⁴⁰ Nevertheless, these features seem to correspond with the hysteresis and remanent moment observed in the magnetization curves throughout the entire AF ordered LTT phase of $\text{La}_{1.8-x}\text{Eu}_{0.2}\text{Sr}_x\text{CuO}_4$ ($x < 0.02$).³³

The LTLO phase, represented by the middle panels in Fig. 8, is expected to show some intermediate behavior. In the temperature range $90 \text{ K} \lesssim T \lesssim 120 \text{ K}$, where this phase assumes 100% volume fraction, it offers a unique opportunity to study the interlayer magneto-transport as a function of $(b - a)$ and $\theta = 2\alpha$. Figure 9(a) shows the temperature dependence of $(b - a)$ and $\Delta\rho_c$ for $H \parallel c$, normalized to their values at T_{LT} . The correct way to

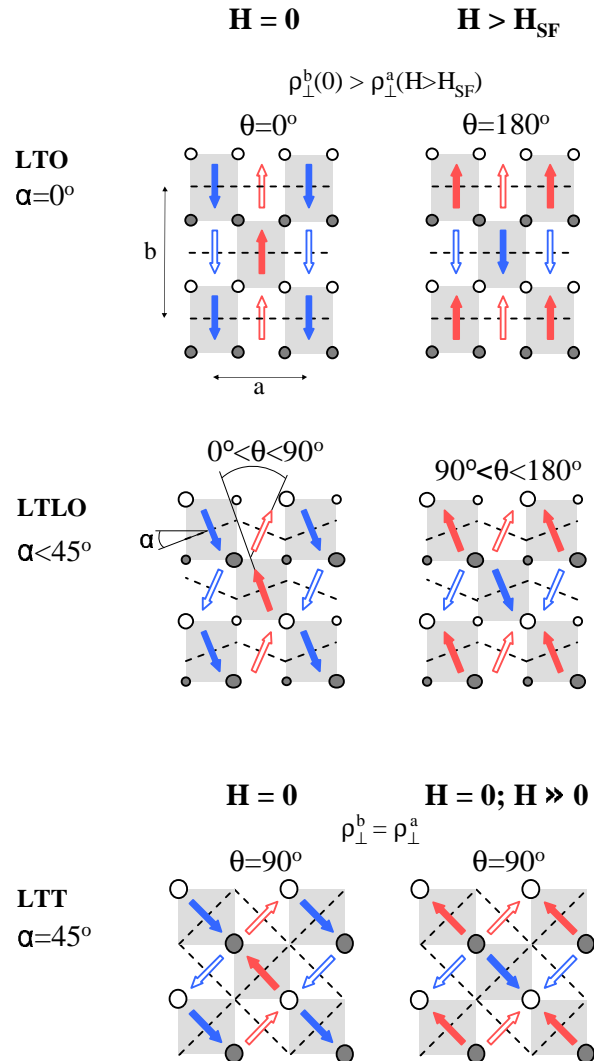


FIG. 8: (color online) Spin structures of two adjacent CuO_2 planes in the LTO, LTLO and LTT phases for zero and high magnetic fields $H \parallel c$. Closed spins and gray plaquettes form one plane, open spins and white plaquettes the other. White (gray) oxygen atoms are displaced above (below) the CuO_2 plane. The size of the circles grows with displacement. Dashed lines indicate the octahedral tilt axes. Spin canting is coupled to the octahedral buckling pattern, although canting angles ($\lesssim 0.2^\circ$) are much smaller than tilt angles ($\lesssim 5^\circ$). Spins pointing towards white (gray) oxygen atoms are canted out of the plane (into the plane) of the paper. ρ_\perp^a and ρ_\perp^b symbolically denote the microscopic (not macroscopically measured) interlayer hopping resistance in a and b direction.

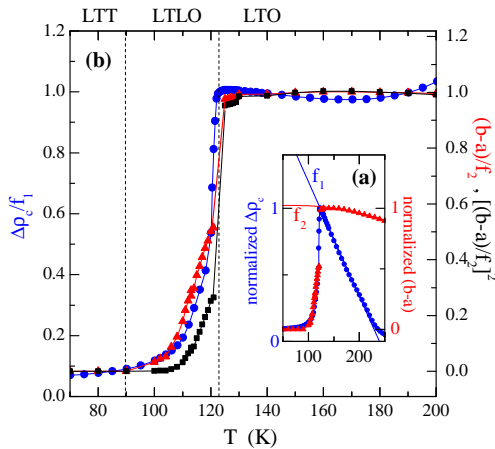


FIG. 9: (color online) Temperature dependence of the magneto-resistance $\Delta\rho_c$ and strain $(b-a)$ in the LTLO phase. (a) $\Delta\rho_c$ (blue circles) and $(b-a)$ (red triangles) normalized at T_{LT} . f_1 and f_2 are extrapolations of the data in the LTO phase to $T < T_{LT}$. (b) Same properties as in (a) divided by f_1 and f_2 . The square of $(b-a)/f_2$ is plotted as well (black squares). In the case of the x-ray results only single phase data points are shown.

compare these properties is after division by their values in the LTO phase, extrapolated into the LTT phase; see functions f_1 and f_2 . The result is shown in Fig. 9(b). Several scenarios are possible. If $\Delta\rho_c$ (blue circles) depends primarily on the spin orientation θ , then it should be proportional to $\cos(\theta) \propto (b-a)$ (red triangles). However, it is more likely that $\Delta\rho_c$ also depends on the orthorhombic strain, which produces the anisotropy of the interlayer hopping along a and b in first place, so that one may expect $\Delta\rho_c$ to be in first approximation proportional to $(b-a) \cdot \cos(\theta) \propto (b-a)^2$ (black squares). The similarity between the temperature dependencies of $\Delta\rho_c$ and $(b-a)^q$ clearly shows that these quantities are connected. Within the experimental error of the independent x-ray diffraction and magneto-resistance measurements it is, however, not possible to decide on the exponent q . To isolate the effects of $(b-a)$ and θ on $\Delta\rho_c$, one could study the magneto-resistance in the LTO phase under pressure. Pressure is known to reduce the orthorhombic strain.

What has been learned that may apply to the stripe ordered LTT phase of $\text{La}_{2-x}\text{Ba}_x\text{CuO}_4$? The stripe phase consists of spin stripes coupled antiphase across the charge stripes (Fig. 3 in Ref. 41). The stripe direction is parallel to the Cu-O-Cu bond but rotates by 90° in adjacent planes, similar to the octahedral tilt axes. In zero field spins are parallel to the stripes, resulting in a non-collinear spin structure ($\theta = 90^\circ$). It is easy to see that for this type of system a large normal state c -

axis magneto-resistance may not be observed for any field direction. First the tetragonal symmetry offers no advantage for any interlayer hopping direction. Second in terms of the simple hopping picture often applied to the lightly doped compounds, i.e., hole and spin swap sites, interlayer hopping in the stripe phase always creates frustrated spin moments between antiphase spin stripes. The application of a high magnetic field $H \parallel c$ was shown to have no effect on the magnetic order.⁴¹ Even if spin stripes carry a WFM due to DM superexchange (which is still unknown) the net WFM of each plane cancels out because of the phase shift by π across charge stripes. Hence, no spin-flip transition can be induced, ruling out a similarly strong c -axis magneto-resistance as in the AF ordered LTO phase of the lightly doped compounds. Application of a high magnetic field parallel to the CuO_2 planes produces a collinear spin structure, i.e., spins within the stripes rotate until they are approximately perpendicular to the field.⁴¹ However the stripes themselves do not rotate. Thus, even if slight lattice distortions due to, e.g., the charge stripes would lift the structural frustration, the topology of the interlayer superexchange for a collinear spin configuration compares to a checkerboard pattern with $\theta = 0^\circ$ and $\theta = 180^\circ$. As discussed in Refs. 15,16,17, this indeed perfect magnetic and electronic decoupling of the planes seems responsible for the frustration of the interlayer Josephson coupling and the concomitant loss of 3D superconducting phase coherence.

In summary, the magneto-transport of lightly hole doped $\text{La}_{1.79}\text{Eu}_{0.2}\text{Sr}_{0.01}\text{CuO}_4$ has been explored and linked to structural and magnetic properties. It was shown that the low temperature structural transition from orthorhombic to tetragonal symmetry and from collinear to non-collinear spin structure eliminates the spin-valve type contribution to the interlayer magneto-resistance. After calculating out spin orientation dependent effects by averaging high and low field data, the interlayer transport appears largely unaffected by the structural transition. In contrast, the transition triggers a significant increase of the in-plane charge carrier localization.

V. ACKNOWLEDGEMENT

The author thanks J. M. Tranquada for fruitful discussions, and P. Reutler and G. Dhalenne for support during the crystal growth experiment at the Laboratoire de Physico-Chimie de l'Etat Solide in Orsay. The work at Brookhaven was supported by the Office of Science, U.S. Department of Energy under Contract No. DE-AC02-98CH10886.

¹ N. W. Preyer, R. J. Birgeneau, C. Y. Chen, D. R. Gabbe, H. P. Jenssen, M. A. Kastner, P. J. Picone and T. Thio.

Phys. Rev. B **39**, 11563 (1989).

² T. Thio, T. R. Thurston, N. W. Preyer, P. J. Picone, M. A.

- Kastner, H. P. Jenssen, D. R. Gabbe, C. Y. Chen, R. J. Birgeneau and A. Aharony. *Phys. Rev. B* **38**, 905 (1988).
- ³ T. Thio, C. Y. Chen, B. S. Freer, D. R. Gabbe, H. P. Jenssen, M. A. Kastner, P. J. Picone, N. W. Preyer and R. J. Birgeneau. *Phys. Rev. B* **41**, 231 (1990).
- ⁴ N. D. Mermin and H. Wagner. *Phys. Rev. Lett.* **17**, 1133 (1966).
- ⁵ A. Gozar, B. S. Dennis and G. Blumberg. *Phys. Rev. Lett.* **93**, 027001 (2004).
- ⁶ M. Hücker, H.-H. Klauss and B. Büchner. *Phys. Rev. B* **70**, R220507 (2004).
- ⁷ L. Shekhtman, I. Ya. Korenblit and A. Aharony. *Phys. Rev. B* **49**, 7080 (1994).
- ⁸ L. Benfatto and M. B. Silva Neto. *Phys. Rev. B* **74**, 024415 (2006).
- ⁹ H. E. Viertiö and N. E. Bonesteel. *Phys. Rev. B* **49**, 6088 (1994).
- ¹⁰ A. R. Moodenbaugh, Y. Xu, M. Suenaga, T. J. Folkerts and R. N. Shelton. *Phys. Rev. B* **38**, 4596 (1988).
- ¹¹ J. M. Tranquada, B. J. Sternlieb, J. D. Axe, Y. Nakamura and S. Uchida. *Nature* **375**, 561 (1995).
- ¹² M. Fujita, H. Goka, K. Yamada, J. M. Tranquada and L. P. Regnault. *Phys. Rev. B* **70**, 104517 (2004).
- ¹³ Y. Maeno, N. Kakehi, M. Kato and T. Fujita. *Phys. Rev. B* **44**, 7753 (1991).
- ¹⁴ J. D. Axe, A. H. Moudden, D. Hohlwein, D. E. Cox, K. M. Mohanty, A. R. Moodenbaugh and Y. Xu. *Phys. Rev. Lett.* **62**, 2751 (1989).
- ¹⁵ Q. Li, M. Hücker, G. D. Gu, A. M. Tsvelik and J. M. Tranquada. *Phys. Rev. Lett.* **99**, 67001 (2007).
- ¹⁶ E. Berg, E. Fradkin, E.-A. Kim, S. A. Kivelson, V. Oganessian, J. M. Tranquada and S. C. Zhang. *Phys. Rev. Lett.* **99**, 127003 (2007).
- ¹⁷ J. M. Tranquada, G. D. Gu, M. Hücker, H.-J. Kang, R. Klingeler, Q. Li, J. S. Wen, G. Y. Xu, Z. J. Xu and M. v. Zimmermann. arXiv:0809.0711 (2008).
- ¹⁸ A. V. Chubukov and A. M. Tsvelik. *Phys. Rev. B* **76**, 100509 (2007).
- ¹⁹ J. F. Ding, X. Q. Xiang, Y. Q. Zhang, H. Liu and X. G. Li. *Phys. Rev. B* **77**, 214524 (2008).
- ²⁰ M. Matsuda, M. Fujita, K. Yamada, R. J. Birgeneau, Y. Endoh and G. Shirane. *Phys. Rev. B* **65**, 134515 (2002).
- ²¹ T. Thio and A. Aharony. *Phys. Rev. Lett.* **73**, 894 (1994).
- ²² Y. Ando, A. N. Lavrov and S. Komiya. *Phys. Rev. Lett.* **90**, 247003 (2003).
- ²³ M. Hücker, M. v. Zimmermann, R. Klingeler, S. Kiele, J. Geck, S. Bache, J. P. Hill, A. Revcolevschi, D. J. Buttrey, B. Büchner and J. M. Tranquada. *Phys. Rev. B* **74**, 85112 (2006).
- ²⁴ In $\text{La}_{1.99}\text{Sr}_{0.01}\text{CuO}_4$ this transition occurs at $T_{\text{HT}} \simeq 500$ K. For $\text{La}_{1.79}\text{Eu}_{0.2}\text{Sr}_{0.01}\text{CuO}_4$ we estimate that $T_{\text{HT}} \simeq 680$ K, based on our experience that T_{HT} increases approximately 9 K per 0.01 Eu.
- ²⁵ P. Böni, J. D. Axe, G. Shirane, R. J. Birgeneau, D. R. Gabbe, H. P. Jenssen, M. A. Kastner, C. J. Peters, P. J. Picone and T. R. Thurston. *Phys. Rev. B* **38**, 185 (1988).
- ²⁶ P.G. Radaelli, J.D. Jorgensen, R. Kleb, B.A. Hunter, F.C. Chou and D.C. Johnston. *Phys. Rev. B* **49**, 6239 (1994).
- ²⁷ M. K. Crawford, R. L. Harlow, E. M. McCarron, W. E. Farneth, J. D. Axe, H. Chou and Q. Huang. *Phys. Rev. B* **44**, 7749 (1991).
- ²⁸ B. Büchner, M. Breuer, A. Freimuth and A. P. Kampf. *Phys. Rev. Lett.* **73**, 1841 (1994).
- ²⁹ B. Simović, M. Hücker, P. C. Hammel, B. Büchner, U. Ammerahl and A. Revcolevschi. *Phys. Rev. B* **67**, 224508 (2003).
- ³⁰ B. Keimer, R. J. Birgeneau, A. Cassanho, Y. Endoh, M. Greven, M. A. Kastner and G. Shirane. *Z. Phys. B* **91**, 373 (1993).
- ³¹ B. Büchner, M. Breuer, W. Schlabitz, A. Fiack, W. Schäfer, A. Freimuth and A. P. Kampf. *Physica C* **235–240**, 281 (1994).
- ³² S. Ono, S. Komiya, A. N. Lavrov and Y. Ando. *Phys. Rev. B* **70**, 184527 (2004).
- ³³ M. Hücker, V. Kataev, J. Pommer, U. Ammerahl, A. Revcolevschi, J. M. Tranquada and B. Büchner. *Phys. Rev. B* **70**, 214515 (2004).
- ³⁴ A. Lacerda and T. Graf. *Physica C* **235–240**, 1353 (1994).
- ³⁵ V. N. Kotov, O. P. Sushkov, M. B. Silva Neto, L. Benfatto and A. H. Castro Neto. *Phys. Rev. B* **76**, 224512 (2007).
- ³⁶ S.-W. Cheong, J. D. Thompson and Z. Fisk. *Physica C* **158**, 109 (1989).
- ³⁷ K. V. Tabunshchik and R. J. Gooding. *Phys. Rev. B* **71**, 214418 (2005).
- ³⁸ N. E. Bonesteel. *Phys. Rev. B* **47**, 11302 (1993).
- ³⁹ The $M(H)$ curves in the LTT phase are still poorly understood. There is no sharp spin-flip, as well as no spontaneous weak ferromagnetism ($H_{\text{SF}} \sim 0$ T). Although in the low field regime dM/dH is significantly larger than in the LTO phase, which indicates that the AF interlayer coupling is much weaker, it still takes very high fields (> 5 T) to ferromagnetically align all WFM. Let us describe the AF order of the LTO phase as $ududududududududud$, where d and u means WFM moment up and down. Then, the zero field ground state of the LTT phase may possibly look like $uuddduddduuuddudud$. There are random stacks with $udud$, uuu and ddd of different length. The size of these domains is likely to vary also in the ab plane, and will most likely be smaller than in the LTO phase (due to the first order nature of the LTO \leftrightarrow LTLO transition). This may cause a broad distribution of local critical fields and, thus, smear out the spin-flip to a degree that the $M(H)$ curves become effectively linear in a wide field range.
- ⁴⁰ Y. Zhu, A. R. Moodenbaugh, Z. X. Cai, J. Taftø, M. Suenaga and D. O. Welch. *Phys. Rev. Lett.* **73**, 3026 (1994).
- ⁴¹ M. Hücker, G. D. Gu and J. M. Tranquada. cond-mat/0503417 (2005).